Int. J. Electrochem. Sci., 7 **(2012)** 6677 - 6692

International Journal of
ELECTROCHEMICAL
SCIENCE
www.electrochemsci.org

Influence of Heat and Laser Treatments on the Corrodibility of the Reinforced Carbon Steel

G. A. El-Mahdy[1,2,], M. M. Hegazy[1], M. M. Eissa[3], A. M. Fathy[3], F. M. Sayed,[1] N. El-Manakhly[4] and Hamad –Al-Lohedan[2]*

[1] Chemistry Department, Faculty of Science, Helwan University, Cairo, Egypt
[2] Surfactants research Chair, Chemistry Department, College of Science, King Saud University, P.O.Box - 2455, Riyadh - 11451, Saudi Arabia
[3] Steel Technology Department – Central Metallurgical Research & Development Institute (CMRDI)
[4] Electrochemistry and Corrosion lab., National Research Centre (NRC), Egypt.
[*]E-mail: gamalmah2000@yahoo.com

Received: 5 July 2012 / *Accepted:* 16 July 2012 / *Published:* 1 August 2012

The influence of heat and laser treatments on the corrosion behavior of reinforced carbon steel was investigated in calcium hydroxide solution using weight loss, photodynamic polarization measurements, X-ray diffraction (XRD) and Scanning Electron Microscope (SEM). Heat and laser treatments play an important role for improvement of the mechanical and corrosion resistance of the reinforced carbon steel. The corrosion rate of laser alloyed sample is very close to that of the sample treated with low heat treatment (900 ^{o}C) and is lower than that experienced for the sample treated at higher one (1200 ^{o}C). The results may be attributed to uneven distribution of Ti and V micro-alloying element throughout the surface and low grain refinement for treated sample at high heat treatment (1200 ^{o}C).

Keywords: Heat treatment, Laser, Micro-alloyed steel, Titanium, Vanadium, XRD, Polarization, SEM

1. INTRODUCTION

Construction and design problems have led to an early deterioration of concrete structures, reducing their residual service life as the infrastructure is aged in a corrosive environment. Corrosion of reinforcement steels is one of the main causes for the deterioration [1,2] and pitting corrosion of reinforcement steels and is considered as the most disastrous form of corrosion due to an extremely difficult to be predicted [3]. A lot of work has been done to investigate compositions of different types of concrete and their effect on the corrosion behavior of steels [4–12] and the electrochemical

behavior of reinforcing steel in simulated concrete pore conditions in $Ca(OH)_2$ solutions [10,13-14]. Several work have been also carried out using a mixture of $Ca(OH)_2$, Na(OH) and K(OH) solutions [15,16] containing different ions such as Na^+, K^+ and $(SO4)^{2-}$ depending on the type of cement and supplementary cementing materials [5,12]. Electrochemical measurement such as potentiodynamic polarization was widely used for studying corrosion behavior of carbon steels in different solutions [16,17–21]. A little work has been done to improve the mechanical properties and corrosion resistance of reinforcing steel by dual phase heat treatment [22-24]. Laser surface melting has various advantageous as homogenization, dissolution of the precipitated or segregated phases and rapid quenching from the melt leading to fine microstructure and consequently improvement of the mechanical and corrosion resistance properties. There is growing interest in application of laser melting in carbon steel aimed at enhancing mechanical and corrosion resistance properties [25-30]. In our recent preceding paper [31] on this research, it was found with experimental results that an improvement in the corrosion resistant was achieved by micro-alloying additions of titanium (Ti) and vanadium (V) to reinforced carbon steel. In present work, the influence of heat and laser treatments on the microstructure and corrodibility of the reinforced carbon steel will be investigated using weight loss, potentiodynamic polarization measurements, XRD and SEM analysis.

2. EXPERMENTAL

2.1 Chemical composition

Table (1) represents the chemical composition of investigated heat treated steels. Ti and V were added as micro-alloying elements to improve the mechanical and electrochemical properties.

Table 1. Chemical composition of the investigated non-micro-alloyed (X), V-micro-alloyed (V1, V2) and Ti-micro-alloyed (T1, T2) steels.

Steel	Chemical composition, wt%									
No	C	Mn	Si	P	S	Cr	Ni	Al	V	Ti
X	0.214	0.94	0.26	0.011	0.042	0.112	0.01	0.005	--	--
V1	0.21	1	0.28	0.031	0.033	0.122	0.001	0.003	0.12	--
V2	0.195	1.27	0.32	0.012	0.008	0.053	0.001	0.004	0.22	--
T1	0.214	1.02	0.28	0.022	0.04	0.138	0.087	0.047	--	0.12
T2	0.23	0.98	0.37	0.04	0.02	0.1	0.01	0.1	--	0.2

2.2 Heat and laser treatments

Five samples were selected for heat treatments. One non-micro-alloyed steel (X), two V-micro-alloyed steels, V (with different V-contents) and two Ti-micro-alloyed steels, T (with different Ti-contents). All the specimens subjected to heat treatment process have the same C-content. Two heat

treatments processes were used on the selected five samples. In the first one, the steel samples were reheated to 900^{o}C for 1 hour and followed by quickly quenching in water. The quenched steel samples were then tempered at 600^{o}C for 1 hour and followed by normal air cooling. In the second heat treatment process, the steel samples were reheated to 1200^{o}C for 1hour and followed by quickly quenching in water. The quenched steel samples were then tempered at 600^{o}C for 1 hour and followed by normal air cooling [4]. Three carbon steel samples were selected to apply laser surface hardening. These employed samples are (V2, T1 and T2). The laser surface hardening process had been implemented with Power 3 kW at pressure 0.6 Mpa.

2.3. Weight loss measurements

The weight loss versus time was monitored for Triplicate specimens in aqueous solution of $Ca(OH)_2$+0.6M NaCl adjusted to pH 12 and the average weight loss was determined.

2.4 Materials and test solutions

The area of the steel samples used in weight loss and electrochemical measurements were 0.15 cm^2. They were fitted into glass tubing of appropriate internal diameter by an epoxy resin (Araldite type), leaving only the front surface areas to contact the test solutions. The surface of the electrodes were mechanically polished with emery papers of different grades down to 4/0, degreased with acetone then thoroughly rinsed with bi-distilled water and eventually dried with air. The test solution ($Ca(OH)_2$ solution (pH = 12) containing 0.6 M NaCl was prepared from bi-distilled water and reagent grade chemicals.

2.5 Potentiondynamic polarization measurements

All potentials were measured with respect to a saturated calomel reference electrode (SCE). A spiral platinum electrode with large surface area served as a counter electrode. All electrochemical measurements were performed using VOLTA LAB 40 (Model PGZ301). The polarization resistance R_p and corrosion current will be calculated with the aid of software (VoltaMaster 4 version 7.08).

2.6. X-ray Diffraction (XRD) and SEM analysis

The XRD patterns of the immersed specimens were recorded using a computer controlled X-ray powder diffractometer system, PANALYTICAL X PERTPRO (Holland) with Cu target radiation (Ni filtered, wavelength =1.5418 A°) at a rating of 45 kV, 40 mA. The peak search and search match programs (built in software) were used to identify the peak-table, and ultimately for identification of the peaks. The scan rate was 0.05 - 20° per step and the measuring time was 1 sec. per step.

The film formed on the surface of the specimens after the immersion on the tested solution regions was investigated using scanning electron microscope (SEM). The employed SEM was Jeal

JSM-5410 scanning microscope (Japan). The filament was pre-centered tungsten hairpin type with an accelerating voltage of 3.0 to 30 kV. The energy source was secondary electron and the magnification used is 2000X.

3. RESULTS AND DISCUSSION

3.1. Influence of heat treatments on microstructure of carbon steel

Figure 1 shows the optical microscope examination of quenched-tempered heat treated specimen. It can be seen the presence of martensite microstructure in all investigated reinforced carbon steels. However, it is clear that V (V1and V2) and Ti microalloyed steels (T1and T2) exhibit finer microstructure than non micro-alloyed steel (X) in the same heat treatment condition.

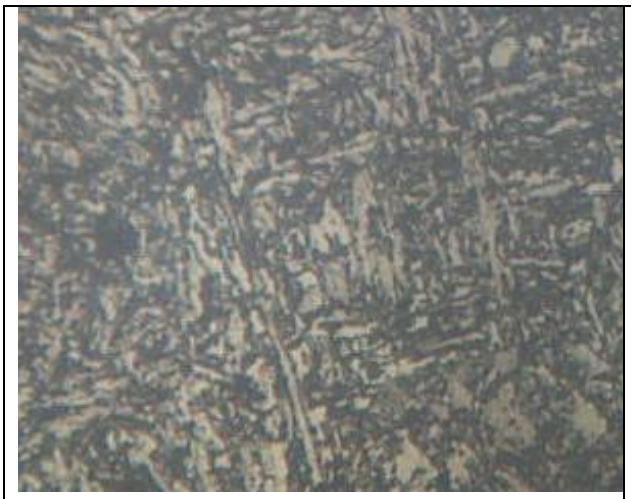

Steel X1 (non-micro-alloyed steel) after HT at (900ºC)

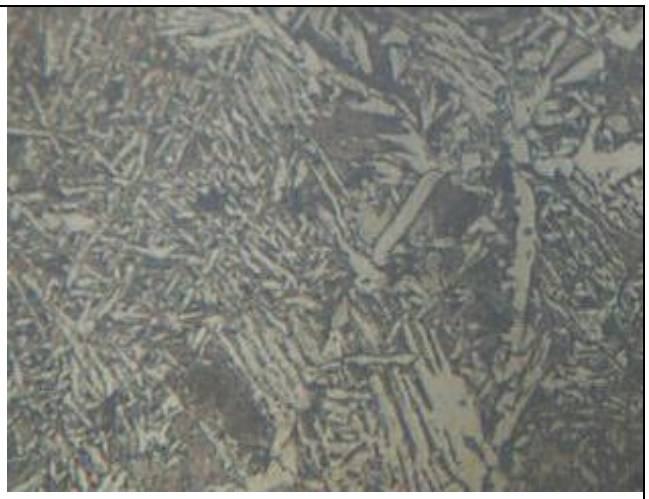

Steel X2 (non-micro-alloyed steel) after HT at (1200ºC)

Steel V1 (V micro-alloyed steel) after HT at (900ºC)

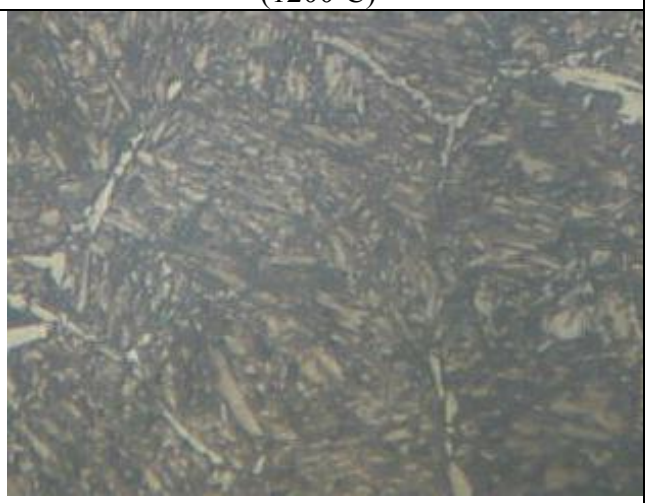

Steel V1 (V micro-alloyed steel) after HT at (1200ºC)

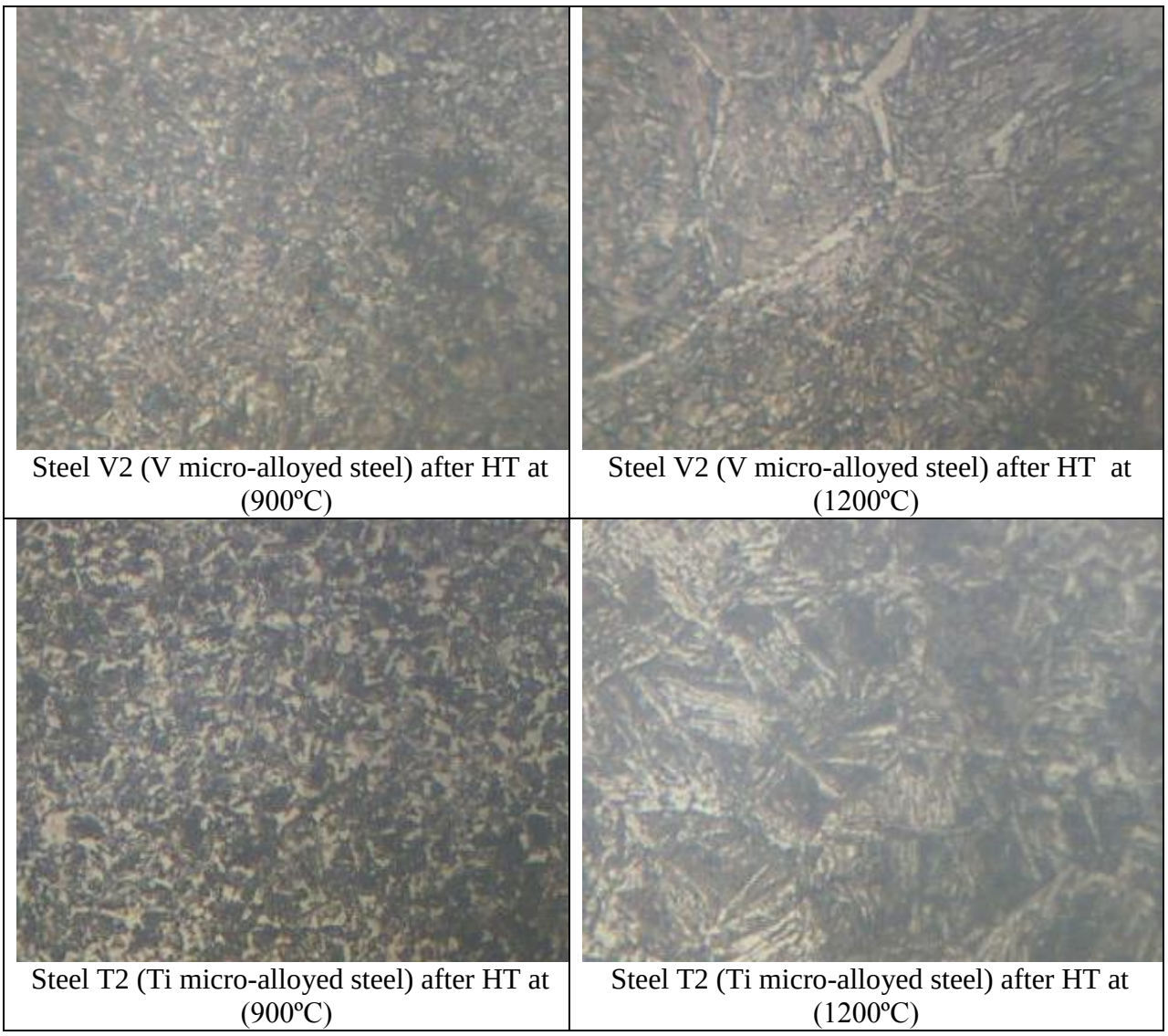

Figure 1. Microstructure of non-micro-alloyed steel (X), V-micro-alloyed steels (V) and Ti-micro-alloyed steel (Ti) after quenching-tempering processes at two different heat treatments: At 900 ^{o}C (X1, V1, T1) At 1200 ^{o}C (X2, V2, T2)

This grain refinement may be attributed to the pinning effect of carbides and nitrides. Moreover, the presence of Ti and V as micro-alloying elements on austenite and inhibition of austenite grain growth during austenitizing process enhance the grain refinement. It can be concluded that the heat treatment assist the grain refinement for the same micro-alloying composition of carbon steel.

3.2 Monitoring of the weight loss at different heat treatments

Figures 2-4 show the monitoring data of the mass loss vs. time for examined carbon steel samples immersed in aqueous solution of $Ca(OH)_2$ + 0.6M NaCl at pH 12 before heat treatment, after heat treatment at 900 ^{o}C and at 1200 ^{o}C, respectively. It is clear that the mass loss of the sample decreases in the following order: before heat treatment > after heat treatment at 1200 ^{o}C > after heat

treatment at 900 ^{o}C. The corrosion rate of the samples was calculated at the different conditions and quoted in table (2).

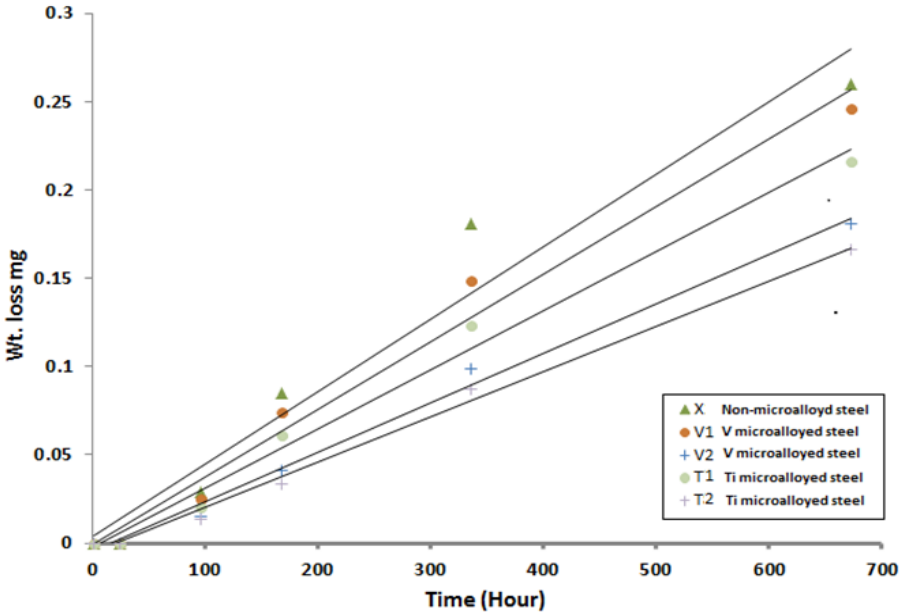

Figure 2. Monitoring data of the weight loss versus immersion time before heat treatment for non-micro-alloyed (X) V-micro-alloyed steels (V) and Ti-micro-alloyed (Ti) carbon steel immersed in $Ca(OH)_2$ solution +0.6M NaCl at pH 12.

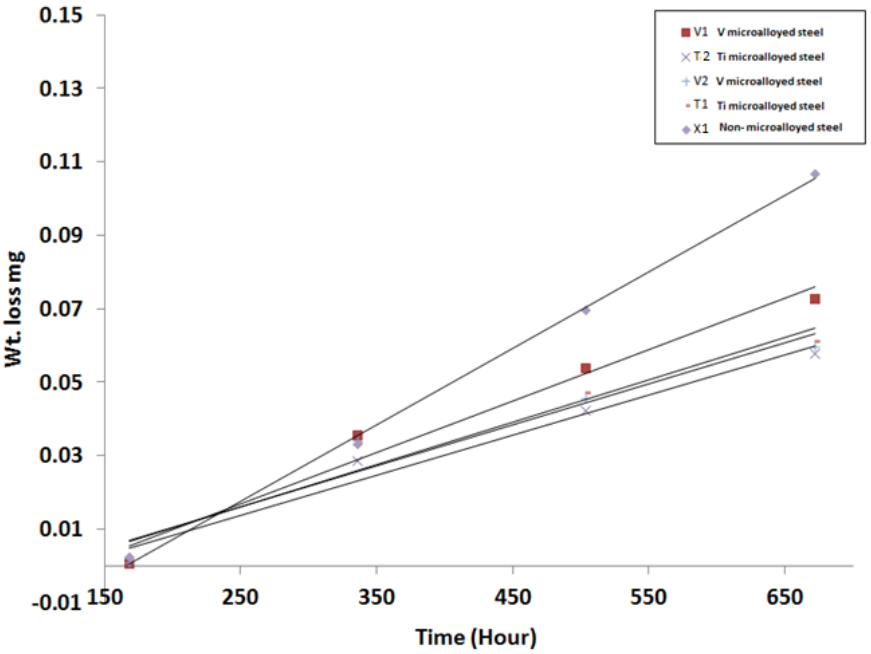

Figure 3. Monitoring data of the weight loss versus immersion time after heat treatment at 900 ^{o}C for non-micro-alloyed (X) V-micro-alloyed steels (V) and Ti-micro-alloyed (Ti) carbon steel immersed in $Ca(OH)_2$ solution +0.6M NaCl at pH 12.

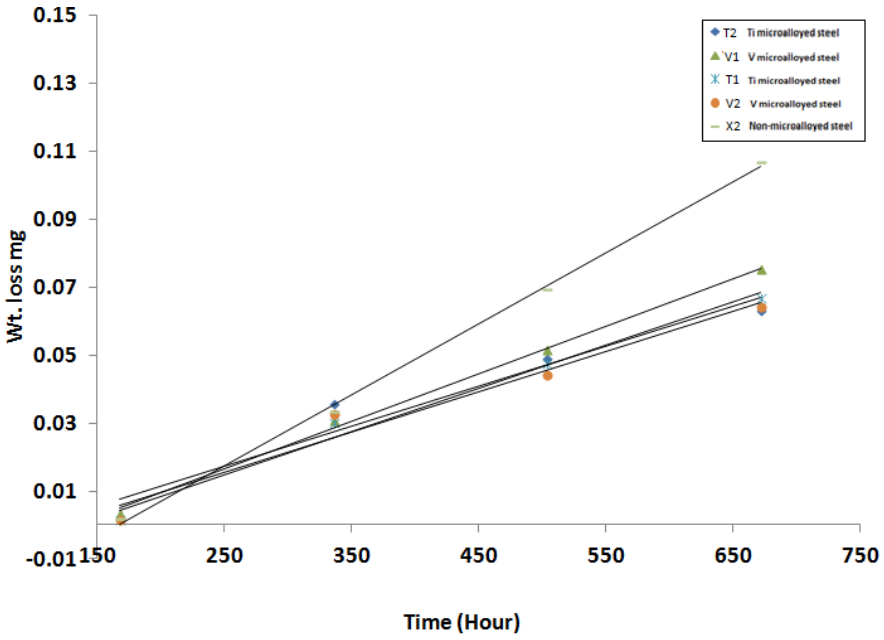

Figure 4. Monitoring data of the weight loss versus immersion time after heat treatment at 1200 ^{o}C for non-micro-alloyed (X) V-micro-alloyed steels (V) and Ti-micro-alloyed (Ti) carbon steel immersed in $Ca(OH)_2$ solution +0.6M NaCl at pH 12

Table 2. Corrosion rate for of the investigated non-micro-alloyed (X1 and X2), V-micro-alloyed (V1, V2) and Ti-micro-alloyed (T1, T2) steels in $Ca(OH)_2$ + 0.6 M NaCl at pH=12 at different heat treatments.

	Sample	Corrosion rate mg/y
X	(X1) HT at 900ºC	0.0349
	(X2) HT at 1200ºC	0.0351
V1	HT at 900ºC	0.0235
	HT at 1200ºC	0.0236
V2	HT at 900ºC	0.0187
	HT at 1200ºC	0.020
T1	HT at 900ºC	0.0193
	HT at 1200ºC	0.0213
T2	HT at 900ºC	0.0184
	HT at 1200ºC	0.0198

It is interesting to note that the alloyed surface is highly sensitive to heat treatment. The higher corrosion rate experienced by the untreated specimen can be attributed to the low grain refinement. The results showed that the resistance of reinforced steel to corrosion for the sample treated at high heat treatment (1200 ^{o}C) is substantially higher than that treated at low one (900 ^{o}C). It was concluded that the treatment of the sample at low heat treatment is accompanied by an increase in ductility of the surface layer, which in turn improve the resistance of the specimen to corrosion, since a more ductile surface layer is less sensitive to the action of corrosive media. Moreover, the addition of micro-

alloyimg elements like V and Ti to the reinforced carbon steel is playing an important role in the improvement of the mechanical properties and corrosion resistance of the micro-alloyed carbon steel. V and Ti additions enhance the grain size refinement, which is the main factor of decreasing the corrosion rate of the micro-alloyed carbon steel samples. The micro-addition of V is a good aspect of alloying elements of the steel. It exists on crystal and grain boundary, which inhibit the grain growing and dissolves much less in ferrite than in austenite leading to grain refinement. The presence of Ti as micro-alloying element can form a number of compounds that provide grain refinement and strengthening the precipitation. A small amount of Ti is effective to enhance grain refinement in reheated or continually cast steels since; it retards the grain growth of re-crystallized austenite.

3.3 Influence of heat and laser treatments on potentiodynamic polarization

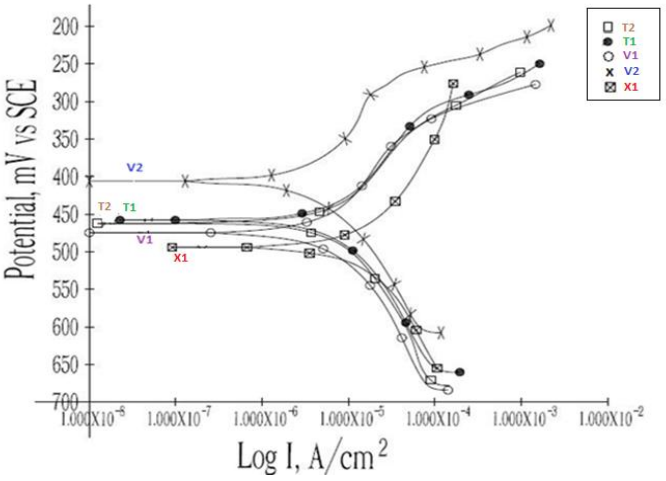

Figure 5. Cathodic and anodic polarization curves for heat treated carbon steel samples at 900°C in saturated $Ca(OH)_2$ solution + 0.6 M NaCl at pH 12.

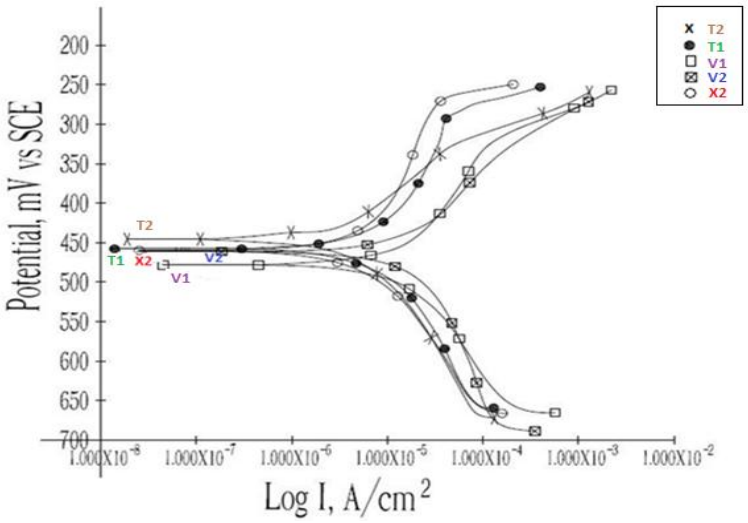

Figure 6. Cathodic and anodic polarization curves for heat treated carbon steel samples at 1200°C in saturated $Ca(OH)_2$ solution + 0.6 M NaCl at pH 12.

The results of cathodic and anodic potentiodynamic polarization curves for untreated sample (US), heat treated sample (HTS) of carbon steel electrodes at 900 and 1200 ^{o}C recorded at scan rate 0.5mVs^{-1} in saturated $Ca(OH)_2$ solution + 0.6 M NaCl at pH 12 are shown in Figs. 5-6, respectively. Samples electrodes were immersed in the test solution for 90 minutes until a steady state potential was attained then anodic polarization was subsequently commenced from the open circuit potential. Generally, all scans exhibit similar performance over the potential domain examined versus SCE. The cathodic curves are almost similar, indicating that the same cathodic reaction takes place on the steel surface. The current in the active region increases with the onset of the anodic polarization due to metal dissolution. The anodic portion of the curve shows an active dissolution with a passive region. The electrochemical dissolution parameters including the corrosion potential ($E_{corr.}$) and the corrosion current density ($I_{corr.}$) were estimated and presented in table 3.

Table 3. Polarization parameters for the investigated non-micro-alloyed (X1 and X2), V-micro-alloyed (V1, V2) and Ti-micro-alloyed (T1, T2) steels in $Ca(OH)_2$ + 0.6 M NaCl at pH=12 at different heat treatments.

Sample		TAFEL CALCULATIONS					
		Corrosion Rate mg/y	I_{corr} μA/cm^2	β anodic V/decade	β cathodic V/decade	E (Inital) mV	E (Final) mV
X	(X1) HT at 900ºC	8.9	19.58	1.65E-01	2.16E-01	-603.5	-393
	(X2) HT at 1200ºC	9.246	20.35	1.00E-01	2.26E-01	-575.5	-371.5
V1	HT at 900ºC	4.831	10.63	1.30E-01	2.09E-01	-575	-373
	HT at 1200ºC	5.477	15.76	1.71E-01	1.71E-01	-599	-357
V2	HT at 900ºC	2.439	5.368	1.90E-01	1.66E-01	-524	-300.5
	HT at 1200ºC	3.598	7.917	2.86E-01	1.82E-01	-589.5	-337.5
T1	HT at 900ºC	1.988	4.375	1.32E-01	6.21E-02	-577.5	-374
	HT at 1200ºC	3.313	7.291	1.83E-01	1.96E-01	-601	-355.5
T2	HT at 900ºC	4.391	9.662	1.24E-01	1.87E-01	-503.5	-348.5
	HT at 1200ºC	4.779	10.52	2.68E-01	2.15E-01	-602	-337.5

It is clear that the untreated specimen (US), has higher corrosion rate than that of HTS. The anodic dissolution current of US, is higher than that of HTS indicating that the dissolution rate was greatly influenced by heat treatment. Therefore, the second phase particles induced by heat treatment seem to be responsible for the lower corrosion rate. The higher corrosion rate experienced by US can be attributed to a larger number of active sites in US and uneven distributions of Ti and V along the surface as well as to low grain refinement. HTS have uniform distributions of Ti and V alloying element with a more refinement of the particles. The corrosion rate observed for the treated specimen at high heat treatment (1200 ^{o}C) is higher than that experienced at low heat treatment (900 ^{o}C). The results may be attributed to the uneven distributions of Ti and V alloying element with a low refinement of the particles due to an increase in the degree of Ti and V particles overlap. It can be

concluded that the corrosion rate of steel samples austenized at 1200°C is higher than that of steel samples austenized at 900°C. The results indicated clearly that $E_{corr.}$ shifts towards more negative and the rate of corrosion I_{corr} increases with increasing the heat of treatment. The presence of V and Ti as micro-alloying elements decreases the corrosion rate of carbon steel, while the influence of Ti addition is more effective than the influence of V addition. The micro-addition of V increases the strength, hardness, creep resistance, impact resistance due to formation of hard vanadium carbides and reducing the grain size of the steel. The main advantageous of the micro-addition of Ti as an alloying element in steel is carbide stabilization. It combines with carbon to form titanium carbides, which are quite stable and hard to dissolve in steel and tends to minimize the occurrence of inter-granular corrosion. It may be expected that the corrosion resistance of reinforced carbon steel in calcium hydroxide solution should be increased in presence of Ti and V as micro-alloying elements due to passivating – promoting action of these elements. The length of passive region for the different samples decreases in the following order: HTS at 900 ^{o}C > HTS at 1200 ^{o}C > US. In addition, the polarization resistance, which is proportional to the inverse of the instantaneous corrosion rate, decreases with an increase in heat treatment.

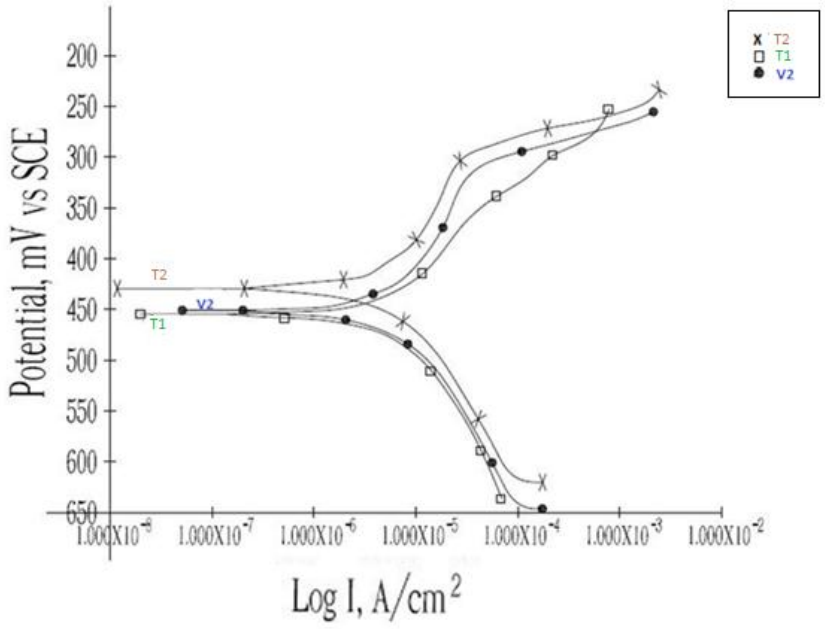

Figure 7. Cathodic and anodic polarization curves for laser treated carbon steel samples immersed in saturated $Ca(OH)_2$ solution + 0.6 M NaCl at pH 12.

The results of heat treatment indicated that the corrosion resistance of the carbon steel is substantially improved by heat treatment are in good agreement with the results reported in the literature for an improvement of the corrosion resistance of the carbon steel with heat treatment due to its improvement of the micro-hardness of carbon steel with heat treatments [22-24, 32-33].

The presence of chloride ions is the major factor, which causes the occurrence of corrosion of reinforces carbon steel in concrete. It was reported previously that the corrosion rate of steels is enhanced by chloride ions, and the effects of chloride ions on carbon steel have been studied and different mechanisms have been suggested [34]. The penetration of the chloride ion into the oxide film through pores or defects is easier than other ions. It is widely known that chlorides ions accelerate corrosion rate of steel obviously and induces the corrosion of reinforcing steel in concrete by causing breakdown of the passive film on the steel surface [35]. Chlorides may be introduced into concrete within the mix ingredients of concrete (e.g. aggregates), or by the use of a chloride-containing admixture (e.g. calcium chloride as an accelerator) or saline water as mixing water (when fresh water is not available). Chlorides in concrete most often come also from the service environment to which the concrete structure is exposed (e.g., exposure to marine environment) [36].

The corrosion rate of laser treated surface (LTS) sample is lower than that of the untreated surface (US) . Fig. 7 indicates that the corrosion and the passivation behavior were similar to that of HTS sample treated at low heat treatment (900 ^{o}C). However transpassive potential of LTS is lower that that of HTS sample treated at low heat treatment (900 ^{o}C), which was obviously due to more formation of oxide films for the laser treated specimen. The uniform distributions of Ti and V among the micro-dendrites during laser treatment are responsible for the lower corrosion rate of LTS. The results of laser treatment are in consistent with the results reported previously for an improvement of corrosion resistance with laser treatment of steel [25-30, 37]

The variation of corrosion rate and the corresponding dissolution current are quoted in table 4.

Table 4. Polarization parameters for Laser surface treated Vanadium (V2) micro-alloyed steel and Titanium micro-alloyed steel (T1 and T2) in saturated $Ca(OH)_2$ solution + 0.6M NaCl at pH 12

Sample	Tafel Calculations					
	Corrosion Rate µm/y	I_{corr} µA/cm^2	β anodic V/decade	β cathodic V/decade	E(initial) mV	E(final) mV
V2	2.346	7.819	2.39E-01	1.74E-01	-572	-327
T1	2.476	9.099	1.42E-01	2.03E-01	-567.5	-355
T2	2.046	4.501	1.00E-01	1.00E-01	-506	-332

Table 5. Influence of heat and laser treatments on the Corrosion rate for Vanadium (V2) micro-alloyed steel and Titanium micro-alloyed steel (T1 and T2) in saturated $Ca(OH)_2$ solution + 0.6M NaCl at pH 12

Corrosion rate mg/y	V2	T1	T2
Hot Rolled	3.420	3.290	2.910
Heat Treated Process at 900ºC	2.439	4.391	1.988
Heat Treated Process at 1200ºC	3.598	4.779	3.313
Laser Treated	2.346	2.476	2.046

The data presented in table 5 indicated that the corrosion rate for sample treated at high heat treatment (1200 ^{o}C) is higher than that experienced by sample treated at low heat treatment (900 ^{o}C) and Laser treated specimen. This may be attributed to uneven distributions of Ti and V alloying element with a low grain refinement due to an increase in the degree of Ti and V particles overlap. It was confirmed that that the corrosion resistance of the reinforced carbon steel increases with laser treatment and decreasing the heat treatment.

3.4 Corrosion products analysis

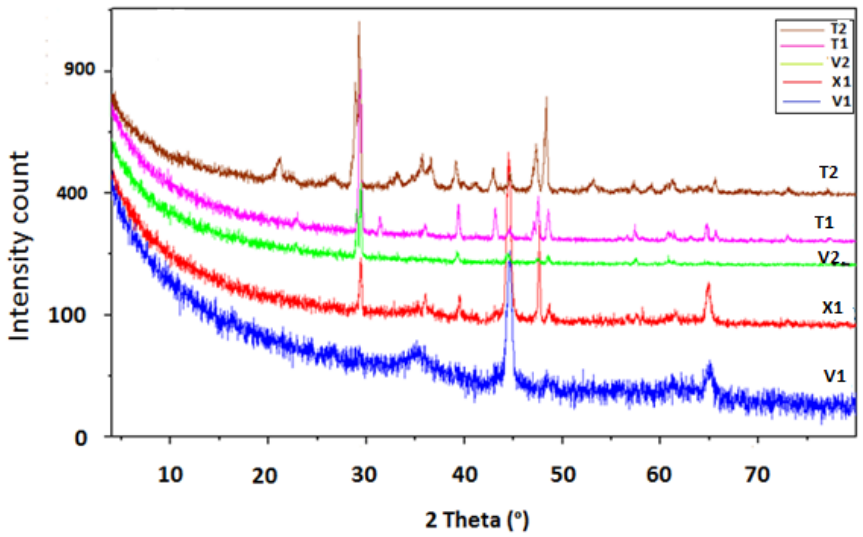

Figure 8. X-ray diffraction patterns for heat treated samples of carbon steel at 900°C after immersion in $Ca(OH)_2$ solution + 0.6 M NaCl at pH =12.

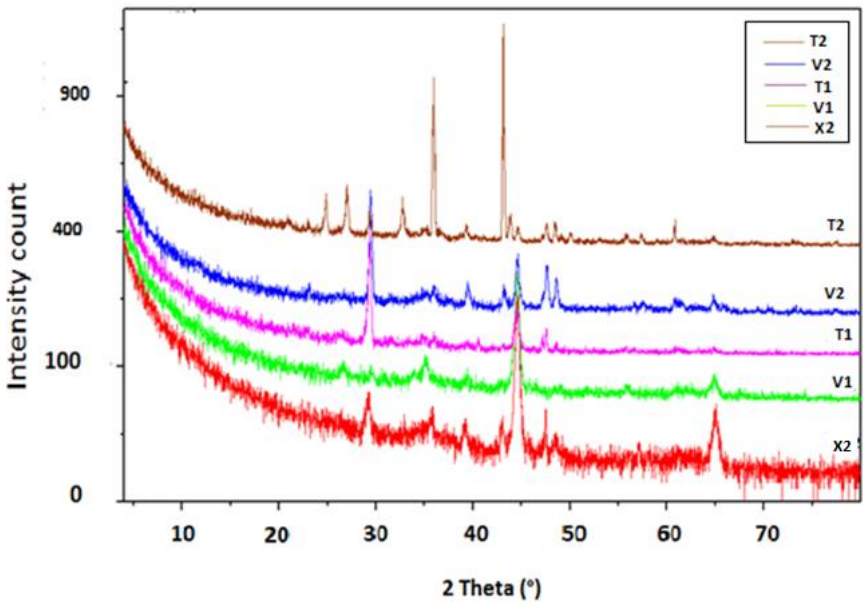

Figure 9. X-ray diffraction patterns for heat treated samples of carbon steel at 1200°C after immersion in $Ca(OH)_2$ solution + 0.6 M NaCl at pH =12.

The chemical compositions of the corrosion products are investigated by XRD for all the examined heat treated micro-alloyed carbon steel samples after immersion in $Ca(OH)_2$ solution + 0.6 M NaCl for 672 hours. Figures 8-9 show the XRD pattern for the heat treated micro-alloyed carbon steel samples at 900 and 1200 ^oC, respectively. XRD data reveals the presence of iron cubic peak with different intensities. The intensity of the iron peak can be arranged in the following order: steel X > steel V > steel T. The results can be attributed to an increase in the amount of iron dissolution and is accompanied by increasing the corrosion rate for the sample treated at high heat treatment 1200 ^oC. The XRD data give an evidence and support for an improvement of the corrosion resistance of the micro-alloyed carbon steel with heat treatments. The lowest corrosion rate experienced by carbon steel alloyed with Ti during heat treatment can be attributed to an increase in the interstitial content of carbon picked up during heat treatment to form carbides and consequent increase in strain hardening and strain rate hardening, which in turn improve the corrosion resistance with het treatment.

X1 (non-micro-alloyed steel) after HT at 900°C

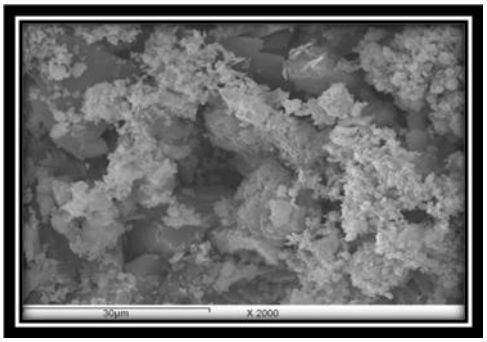

X2 (non-micro-alloyed steel) after HT at 1200°C

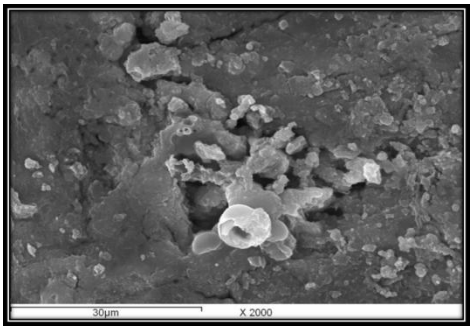

V1 (V micro-alloyed steel) after HT at 900°C

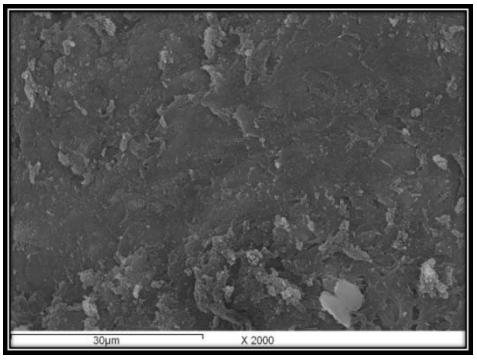

V1 (V micro-alloyed steel) after HT at 1200°C

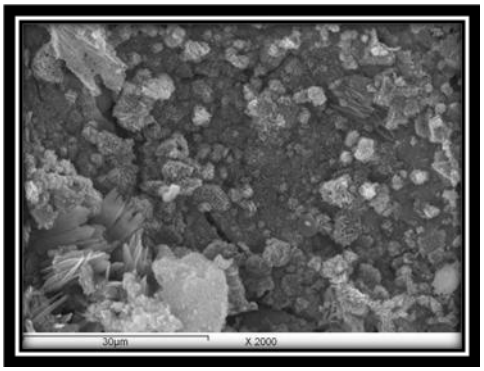

V2 (V micro-alloyed steel) after HT at 900°C

V2 (V micro-alloyed steel) after HT at 1200°C

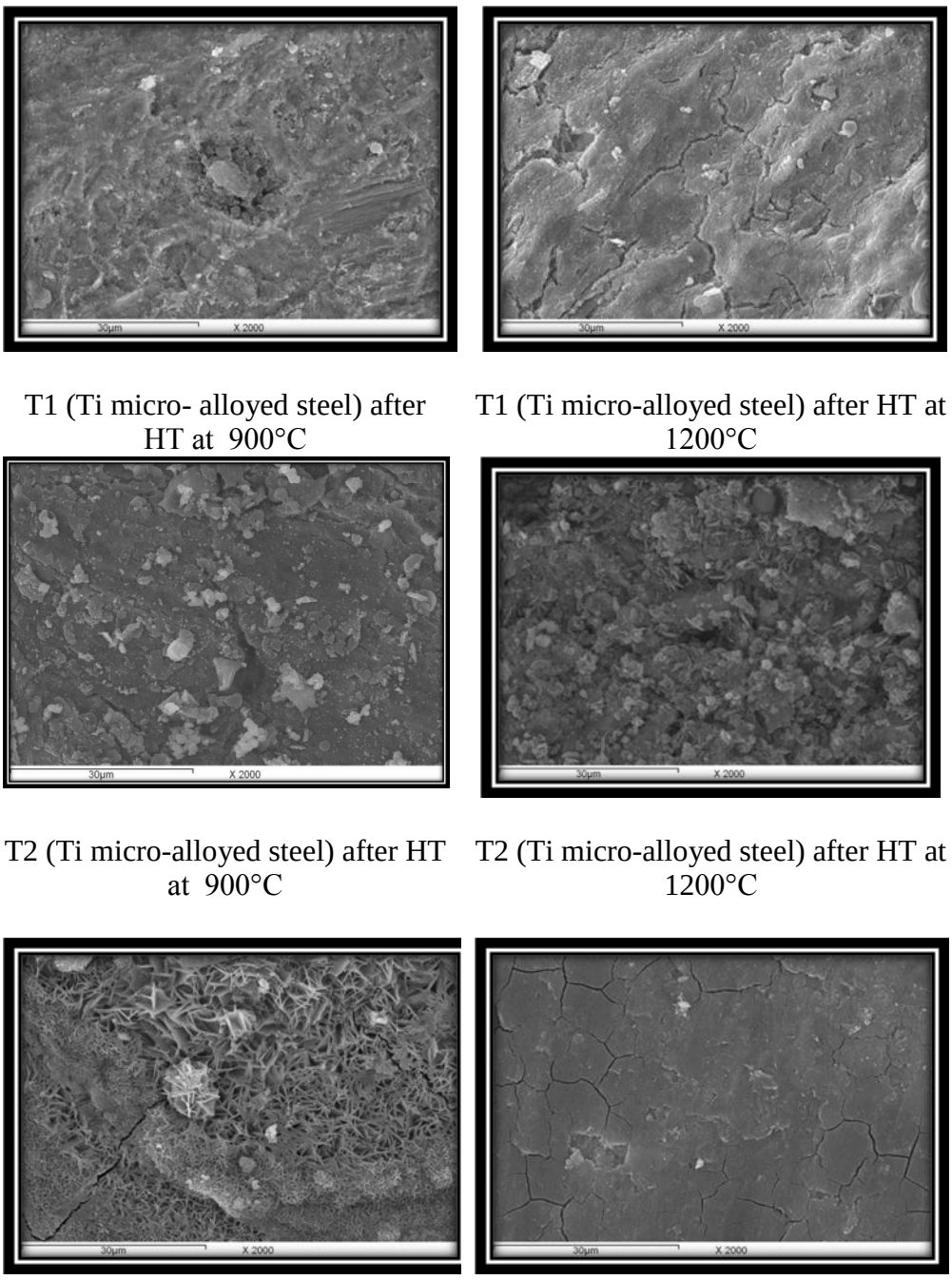

T1 (Ti micro- alloyed steel) after HT at 900°C

T1 (Ti micro-alloyed steel) after HT at 1200°C

T2 (Ti micro-alloyed steel) after HT at 900°C

T2 (Ti micro-alloyed steel) after HT at 1200°C

Figure 10. SEM micrographs for non-micro-alloyed (X) V-micro-alloyed steels (V) and Ti-micro-alloyed (Ti) carbon steel after immersion in $Ca(OH)_2$ solution +0.6M NaCl at pH 12 and heat treatment at two different heat treatments.

Scanning electron microscopy were used to examine the surface of the micro-alloyed heat treated carbon steel samples, which had been naturally immersed for 672 hours in test solution containing $Ca(OH)_2$ solution + 0.6M NaCl at pH =12 . SEM micrographs for the micro-alloyed heat treated carbon steel specimen are presented in figures 10. The micrographs show characteristic inclusion, which probably an oxide film. Also, the surface was damaged strongly and the grain boundaries edges appear clearly. The white areas in the micrograph represent the ferrite phase, while

the dark areas represent mixture of ferrite and cementite (Fe_3C) in a lamellar form (pearlite). It is evident that the attack in the heat treated samples at 900 ^oC is lesser than that experienced by treated sample at high heat treatment 1200 ^oC. It can be seen that the grain size of the sample treated at low heat treatment have a smaller grain size than the samples treated at higher heat treatment at 1200ºC. The micrograph indicates that the grain size of the micro-alloyed carbon steel samples containing Ti and V is smaller than the unalloyed carbon steel samples. Hence, it reduces the grain size and improving the electrochemical behavior of the carbon steel. The attack can be arranged in the in the following order: Steel X > Steel V >Steel T. It can be concluded that the data obtained from the analysis of the corrosion products using XRD and SEM give an evidence and support for the data obtained from the weight loss and polarization measurements for an improvement of the corrosion resistance of the micro-alloyed carbon steel with heat and laser treatments.

4. CONCLUSIONS

1- Heat and laser treatments play an important role for improvement of the mechanical and corrosion resistance of the reinforced carbon steel.

2- The corrosion rate of laser alloyed sample is close to that of the sample treated with low heat treatment (900 ^oC) and is lower than that for the sample treated at high heat treatment (1200 ^oC).

3- Treatment of sample at high heat treatment (1200 ^oC) is accompanied by uneven distribution of Ti and V micro-alloying element throughout the surface and lowering the refinement of the particles.

4- The corrosion products formed on the reinforced carbon steel is loosely bound to the surface, which gives low corrosion protection and allowing the alloy to be actively corroded.

ACKNOWLEDGMENT
This Project was supported by King Saud University, Deanship of Scientific Research, College of Science and Research Center.

References

1. J.P. Broomfield, D.B. Kevin, K. Hladky, *Cem. Conc. Compos.* 24 (2002) 27.
2. J. Rodriguez, L.M. Ortega, J. Casal, *Const. Build. Mater.* 11 (1997) 239.
3. M.N. Boucherit, D. Tebib, *Anti-Corros. Met. Mater.* 52 (2005) 365.
4. C.L. Page, N.R. Short, W.R. Holden, *Cem. Conc. Res.* 16 (1986) 79.
5. A. Moragues, A. Macias, C. Andrade, *Cem. Conc. Res.* 17 (1987) 173.
6. M. Moreno, W. Morris, M.G. Alvarez, G. S. Duffó, *Corros. Sci.* 46 (2004) 2681.
7. S. Goni, C. Andrade, *Cem. Conc. Res.* 20 (1990) 525–539.
8. P. Ghods, O.B. Isgor, G. Mcrae, T. Miller, *Cem. Conc. Compos*. 31 (2009) 2.
9. D.J. Anstice, C.L. Page, M.M. Page *Cem. Conc. Res.*, 35 (2005) 377.
10. M. Saremi, E. Mahallati, *Cem. Conc. Res.* 32 (2002) 1915.
11. F. Schmidt, F.S. Rostasy, *Cem. Conc. Res*. 23 (1993) 1159.
12. K. Andersson, B. Allard, M. Bengtsson, B. Magnusson, *Cem. Conc. Res.* 19 (1989) 327.
13. G. Blanco, A. Bautista, H. Takenouti, *Cem. Conc. Compos* 28 (2006) 212.

14. C. Monticelli, A. Frignani, G. Trabanelli, *Cem. Conc. Res.* 30 (2000) 635.
15. C.J. Kitowski, H.G. Wheat, *Corrosion* 53 (1997) 216–226.
16. X.M. Liu, Z.M. Shi, H.C. Lin, G.L. Song, C.N. Cao, *J. Chin. Soc. Corros. Prot.* 17 (1997) 19.
17. V.A. Alves, C.M.A. Brett, *Electrochim. Acta* 47 (2002) 2081.
18. R.G. Du, R.G. Hu, R.S. Huang, C.J. Lin, *Anal. Chem*. 78 (2006) 3179.
19. E. Sosa, R. Cabrera-Sierra, M.T. Oropeza, F. Hernandez, N. Casillas, R. Tremont, C. Cabrera, I. Gonzalez, *Electrochim. Acta* 48 (2003) 1665.
20. S.L. Wu, Z.D. Cui, G.X. Zhao, M.L. Yan, S.L. Zhu, X.J. Yang, *Appl. Surf. Sci.* 228 (2004) 17.
21. J.M. Zhao, Y. Zuo, *Corros. Eng. Sci. Tech.* 42 (2007) 203.
22. M. Aksoy , A. Esin . *J. Mater. Eng.,* 10 (1988) 281.
23. D. Trejo ,P. Monteiro G. Thomas G, *Cem. Conc. Res.,* 24 (1994)1245.
24. O. Kelestemur , S. Yildiz , *Const. Build. Mater.* 23(2009)78.
25. M. Carbucchio, G. meazza, G. Palom-Barini and G.Sabogna, *J. Mater. Sci.* 18 (1983) 1543.
26. M.F. Ashby and K.E.Easterling *Acta Met.* 32 (1984) 1935.
27. M.F. Ashby and K.E.Easterling *Acta Met.* 34 (1986) 1533.
28. M. Carbucchio and G. PalomBarini , *J. Mater. Sci.* 21 (1986) 75.
29. P. Canova and E.Ramous *J. Mater. Sci.* 21 (1986) 2143.
30. J. M. Pelletier , D. Pergue and F. Fouquet *J. Mater. Sci.* 24 (1989) 4343.
31. G. A. El-Mahdy, Ayman M Atta, M. M. Hegazy, M. M. Eissa, A. M. Fathy, F. M. Sayed A.K.F. Deyab and Hamad –Al-Lohedan, accepted for publication *in Int. J. Electrochem. Sci.* 7 (2012) *(in press).*
32. I. I. Vaselinko, I. P. Vyval and G. V. Karpenko, *F. Khim. Mek. Mater.* 2 (1966) 227.
33. O. Kelesternur , M H. Kelestemur, S. Yildiz, *J. Ir. St. Res., Inter.* 16 (2009) 55.
34.R.E. Melchers and C.Q. Li, *Corrosion,* 65 (2009)554.
35.D.A.Lopeza, T.Perez, S.N.Simison, *Mater. Des.* 24 (2003) 561.
36.J. K. Boah, S. K. Somuah and P. Leblanc, *Corrosion,* 46 (1990) 153.
37.B. Abdolahi, H.R. Shahverdi, M.J. Torkamany, M. Emami, *Appl. Surf. Sci.* 257 (2011) 9921.